

## Arctic oscillation response to the 1991 Pinatubo eruption in the SKYHI general circulation model with a realistic quasi-biennial oscillation

Georgiy Stenchikov,<sup>1</sup> Kevin Hamilton,<sup>2</sup> Alan Robock,<sup>1</sup> V. Ramaswamy,<sup>3</sup> and M. Daniel Schwarzkopf<sup>3</sup>

Received 19 April 2003; revised 1 December 2003; accepted 24 December 2003; published 14 February 2004.

[1] Stratospheric aerosol clouds from large tropical volcanic eruptions can be expected to alter the atmospheric radiative balance for a period of up to several years. Observations following several previous major eruptions suggest that one effect of the radiative perturbations is to cause anomalies in the Northern Hemisphere extratropical winter tropospheric circulation that can be broadly characterized as positive excursions of the Arctic Oscillation (AO). We report on a modeling investigation of the radiative and dynamical mechanisms that may account for the observed AO anomalies following eruptions. We focus on the best observed and strongest 20th century eruption, that of Mt. Pinatubo on 15 June 1991. The impact of the Pinatubo eruption on the climate has been the focus of a number of earlier modeling studies, but all of these previous studies used models with no quasi-biennial oscillation (QBO) in the tropical stratosphere. The QBO is a very prominent feature of interannual variability of tropical stratospheric circulation and could have a profound effect on the global atmospheric response to volcanic radiative forcing. Thus a complete study of the atmospheric variability following volcanic eruptions should include a realistic representation of the tropical QBO. Here we address, for the first time, this important issue. We employed a version of the SKYHI troposphere-stratosphere-mesosphere model that effectively assimilates observed zonal mean winds in the tropical stratosphere to simulate a very realistic QBO. We performed an ensemble of 24 simulations for the period 1 June 1991 to 31 May 1993. These simulations included a realistic prescription of the stratospheric aerosol layer based on satellite observations. These integrations are compared to control integrations with no volcanic aerosol. The model produced a reasonably realistic representation of the positive AO response in boreal winter that is usually observed after major eruptions. Detailed analysis shows that the aerosol perturbations to the tropospheric winter circulation are affected significantly by the phase of the QBO, with a westerly QBO phase in the lower stratosphere resulting in an enhancement of the aerosol effect on the AO. Improved quantification of the QBO effect on climate sensitivity helps to better understand mechanisms of the stratospheric contribution to natural and externally forced climate variability. *INDEX TERMS:* 1620 Global Change:

Climate dynamics (3309); 3362 Meteorology and Atmospheric Dynamics: Stratosphere/troposphere interactions; 3309 Meteorology and Atmospheric Dynamics: Climatology (1620); 3319 Meteorology and Atmospheric Dynamics: General circulation; 8409 Volcanology: Atmospheric effects (0370); *KEYWORDS:* Arctic oscillation, quasi-biennial oscillation, Pinatubo eruption

**Citation:** Stenchikov, G., K. Hamilton, A. Robock, V. Ramaswamy, and M. D. Schwarzkopf (2004), Arctic oscillation response to the 1991 Pinatubo eruption in the SKYHI general circulation model with a realistic quasi-biennial oscillation, *J. Geophys. Res.*, *109*, D03112, doi:10.1029/2003JD003699.

<sup>1</sup>Department of Environmental Sciences, Rutgers University, New Brunswick, New Jersey, USA.

<sup>2</sup>International Pacific Research Center, University of Hawaii, Honolulu, Hawaii, USA.

<sup>3</sup>NOAA Geophysical Fluid Dynamics Laboratory, Princeton University, Princeton, New Jersey, USA.

### 1. Introduction

[2] A number of recent studies have suggested an important role for stratospheric dynamics in intraseasonal, interannual, and longer-term variations of extratropical surface circulation and climate [Perlwitz and Graf, 1995; Thompson and Wallace, 1998; Baldwin and Dunkerton, 1999]. A particular focus has been on the role of the stratosphere in the variations of the Arctic Oscillation (AO). The AO is manifested primarily as a modulation of the zonal mean

pressure gradient and corresponding circumpolar zonal flows. In addition, the AO has a signature in the Atlantic region that is very similar to that of the familiar North Atlantic oscillation [Hurrell, 1995; Hurrell and van Loon, 1997]. A positive AO index corresponds to intensified westerly flow, particularly over the North Atlantic sector, and at the surface this leads to a characteristic warming over northern Eurasia and western/central/southeastern North America and cooling in Middle East and in northeastern North America. Baldwin and Dunkerton [1999] observed that in winter, variations in the AO at the surface tend to be preceded by variations in the vortex strength in the stratosphere; an anomalously strong stratospheric vortex is typically followed by an anomalously positive AO index at the surface. This may be a consequence of downward dynamical influence modulated by large-scale planetary wave propagation. If this is true, then long-term changes in aspects of stratospheric climate forcing (e.g., trends in stratospheric ozone or greenhouse gases) could lead to long-term changes in surface circulation. This is one possible interpretation of the long-term increasing trend in the AO index that has been observed in recent decades [Labitzke and van Loon, 1995; Hurrell and van Loon, 1997; Fyfe et al., 1999; Graf et al., 1998; Thompson and Wallace, 2000; Shindell et al., 2001; Hoerling et al., 2001].

[3] The radiative perturbations that occur after large explosive volcanic eruptions provide a shorter-term natural experiment to study the possible stratospheric influence on tropospheric circulation. Interestingly, such eruptions have been observed to be followed in the next two winters by an anomalously positive AO index [Groisman, 1992; Robock and Mao, 1992, 1995]. Following large volcanic eruptions, the radiative perturbation from stratospheric aerosols exerts a strong influence on the climate system. Volcanic aerosols cool Earth's surface because of reflection of solar radiation and heat the lower stratosphere because of absorption of thermal IR and solar near-IR radiation [Stenchikov et al., 1998]. The mechanism of AO response involves strengthening of the polar night jet, changing planetary wave propagation from the troposphere into the lower stratosphere, as well as a northward shifting of the tropospheric jet and storm tracks [Kodera and Kuroda, 2000a, 2000b; Robinson, 2000; Shindell et al., 2001; Kirchner et al., 1999; Polvani and Kushner, 2002; Stenchikov et al., 2002; Eichelberger and Holton, 2002; Black, 2002; Limpasuvan and Hartmann, 1999; Lorenz and Hartmann, 2003].

[4] Here we study the stratosphere-troposphere interaction forced by the explosive volcanic eruption of the Mt. Pinatubo on 15 June 1991 [McCormick and Veiga, 1992; Bluth et al., 1992; Dutton and Christy, 1992; Minnis et al., 1993; Labitzke, 1994; Randel et al., 1995; Angell, 1997; Andersen et al., 2001]. Radiative forcing caused by Pinatubo aerosols [Kinne et al., 1992; Minnis et al., 1993; Stenchikov et al., 1998; Andersen et al., 2001] resulted in an increase of temperature in the tropical lower stratosphere by about 2–3 K [Labitzke, 1994; Randel et al., 1995; Angell, 1997] and a global surface temperature decrease of 0.5 K [Robock and Mao, 1992, 1995; Kirchner et al., 1999; Hansen et al., 1996, 1999; Kelly et al., 1996; Kelly and Jones, 1999]. The ozone depletion that results from the presence of the stratospheric aerosols also perturbs the radiation [Turco et al., 1993; Schoeberl et al., 1993;

Kinnison et al., 1994; Randel et al., 1995; Rosenfield et al., 1997; Solomon, 1999; Stenchikov et al., 2002; Rozanov et al., 2002].

[5] For the two boreal winters after the Pinatubo eruption, the National Centers for Environmental Prediction (NCEP) reanalysis data (see our earlier study, Stenchikov et al. [2002, Figures 1–2]) show a stronger polar vortex in the lower stratosphere and a positive phase of the AO in the middle troposphere accompanied by a warming pattern at the surface in the middle and high latitudes over North America and Eurasia.

[6] Stenchikov et al. [2002] explored the effect of the Mt. Pinatubo eruption on the AO by forcing a general circulation model (GCM) with the observed radiative forcing from volcanic aerosols and associated ozone depletion. Unfortunately, this model, and all other models that have been applied thus far to this problem [e.g., Kirchner et al., 1999; Ramachandran et al., 2000], had an unrealistically weak interannual variation of mean circulation in the tropical stratosphere. In reality, the interannual variation of stratospheric circulation is profoundly affected by the quasi-biennial oscillation (QBO) of the tropical winds [Angell and Korshover, 1964] that is also thought to have a significant effect on the tropospheric winter circulation in the extratropical Northern Hemisphere [Holton and Tan, 1980, 1982; Dunkerton and Baldwin, 1991, 1999; Hamilton, 2000; Thompson et al., 2001]. In this study we, for the first time, advance earlier modeling studies of the effects of the Pinatubo aerosols using a version of our model that incorporates an imposed realistic tropical QBO to quantify its effect on climate sensitivity to volcanic radiative forcing.

[7] The QBO is a major feature of the equatorial stratospheric variability [Baldwin et al., 2001]. It is associated with quasiperiodic (about 28 months on average) easterly and westerly wind regimes propagating downward from the upper stratosphere to the tropopause. Most GCMs are not able to simulate a spontaneous QBO, and almost all GCM climate studies have been conducted with models without a QBO. Exceptions are the studies of Hamilton [1998] and Bruhwiler and Hamilton [1999], who investigated stratospheric circulation and chemistry as simulated in a version of the SKYHI GCM altered by including an imposed momentum source that forced a somewhat idealized 27-month QBO in the tropical stratosphere.

[8] In the present study we modified the SKYHI model to include an extra “QBO forcing” that nudged the zonal mean zonal winds at low latitudes toward the prevailing zonal wind observations at Singapore from January 1978 to December 1999. We performed ensembles of control integrations with the QBO forcing included for 1978–1999 and also for just 1989–1993. Then we performed ensembles of runs with the QBO forcing and a realistic representation of the radiative effects of the Pinatubo aerosols for June 1991 to May 1993. We also have available for analysis the earlier experiments of Stenchikov et al. [2002], who have control and aerosol runs without the imposed QBO. We will try to determine if there is a systematic difference in the response to the aerosol that can be attributed to the phase of the QBO.

[9] This paper is organized as follows. Section 2 briefly describes the SKYHI GCM and the design of the numerical experiments. The results of simulations, including the effect of the QBO on mean circulation, are presented in section 3.

In section 4 we conduct an empirical orthogonal function (EOF) analysis and discuss the effects in terms of AO indexes. The conclusions are summarized in section 5.

## 2. SKYHI Model and Experimental Setup

[10] SKYHI is a comprehensive finite difference GCM designed at the Geophysical Fluid Dynamics Laboratory to simulate the general circulation of troposphere, stratosphere, and mesosphere [Fels *et al.*, 1980; Hamilton *et al.*, 1995]. It has been used successfully in studies of middle atmospheric phenomena, planetary wave propagation, QBO, and climate change [Mahlman and Umscheid, 1984; Mahlman *et al.*, 1994; Ramaswamy *et al.*, 1996; Hamilton, 1998].

[11] This study uses a version of the SKYHI model with a  $3^\circ \times 3.6^\circ$  latitude-longitude horizontal spatial resolution and 40-level hybrid sigma-pressure grid from the ground to 0.0096 hPa or about 80 km [Fels *et al.*, 1980]. The vertical level spacing increases with height and is about 1.5 km in the lower stratosphere. This version of SKYHI uses predicted clouds [Wetherald and Manabe, 1988]. The model incorporates the shortwave radiative transfer algorithm of Freidenreich and Ramaswamy [1999], with 25 spectral bands calibrated against “benchmark” calculations. It accounts for absorption by CO<sub>2</sub>, H<sub>2</sub>O, O<sub>3</sub>, and O<sub>2</sub>, and Rayleigh scattering. The longwave radiative transfer scheme [Schwarzkopf and Fels, 1991; Schwarzkopf and Ramaswamy, 1999] uses 8 spectral bands and accounts for absorption by H<sub>2</sub>O, CO<sub>2</sub>, O<sub>3</sub>, CH<sub>4</sub>, N<sub>2</sub>O, and CFCs. In this study we also account for aerosol scattering and absorption in the shortwave, and aerosol absorption in the longwave, as in the work of Ramachandran *et al.* [2000]. Zonal mean distributions of aerosol extinction, single scattering albedo, and asymmetry parameter were specifically calculated for SKYHI spectral and spatial resolutions using SAGE II aerosol extinction for 1.02  $\mu\text{m}$ , and CLAES/ISAMS effective radius as in the work of Stenchikov *et al.* [1998] and then prescribed for the entire period of 2-year perturbed simulations as we did in our previous studies [Kirchner *et al.*, 1999; Andronova *et al.*, 1999; Ramachandran *et al.*, 2000; Stenchikov *et al.*, 2002]. Detailed figures showing the evolution of the aerosol distribution are given in these earlier papers, but here it is of interest to note that overall the aerosol starts to decline in the second year following the eruption, so that the aerosol radiative forcing in the second boreal winter (1992–1993) was somewhat weaker in magnitude than in the first winter (1991–1992). A climatological zonal mean ozone distribution [Randel *et al.*, 1999] is used in all SKYHI experiments presented here.

[12] The QBO has a profound effect on the stratospheric circulation in both the tropics and extratropics [Holton and Tan, 1980, 1982; Dunkerton and Baldwin, 1991] (see also the recent reviews by Hamilton [2000] and Baldwin *et al.* [2001]). Hamilton [1998] introduced an idealized (fixed 27-month period) QBO into the SKYHI model via an imposed zonally symmetric zonal momentum forcing in the tropical stratosphere and studied its effect on model climate and variability. In the present experiments a similar implementation of the QBO was adopted, but with the prescribed momentum source now designed to force a realistic QBO time series for the specific calendar dates simulated. For this purpose we used the 22-year series of

observations of stratospheric zonal wind at Singapore (1.4°N, 103.9°E) for the period from January 1978 to December 1999. Specifically a relaxation term is added to the zonal momentum equation at each grid point:

$$\frac{dU(p, \phi, \lambda, t)}{dt} = -\frac{\langle U \rangle - U_{clim}(p, \phi, t) - U_{QBO}(p, \phi, t)}{\tau(p, \phi)}, \quad (1)$$

where  $\langle U \rangle$  is the zonal mean zonal wind,  $p$  is pressure,  $\phi$  is the latitude, and  $\lambda$  is the longitude. The relaxation timescale  $\tau(p, \phi)$  is plotted by Hamilton [1998, Figure 1];  $\tau(p, \phi)$  is as short as 5 days at the equator between about 70 and 12 hPa and grows rapidly with latitude away from the equator and at heights above 12 hPa and below 70 hPa. No relaxation is applied below the 103 hPa level or poleward of 23.5° latitude. Equation (1) constrains only the zonally symmetric component of the zonal wind  $U$  because the right-hand side of equation (1) does not depend on  $\lambda$  and therefore does not directly affect the wave component of the flow. The zonal mean winds are relaxed to a prescribed state that is the sum of the annually varying climatology,  $U_{clim}$ , plus a QBO component that is based on the actual observations of the zonal wind at Singapore. Naujokat [1986] presents a discussion of the Singapore wind data record. Specifically, the term  $U_{clim}$  is a function of pressure, latitude, and time-of-year and is taken from the long-term monthly climatology of zonal wind in the control version of the model described by Hamilton [1998]. The QBO component,  $U_{QBO}$ , is a function of pressure, latitude, and actual date during 1978–1999 and is defined as:

$$U_{QBO}(p, \phi, t) = U_{sing}(p, t) \times e^{-\left(\frac{\phi}{13^\circ}\right)^2}, \quad (2)$$

where  $U_{sing}$  is a smoothed version of the deseasonalized monthly mean Singapore zonal wind observations. The smoothing was done by a low-pass filtering that retains only periods greater than 6 months. This approach was adopted so that the prescribed wind near the equator would be close to the actual observations on any given date but would blend smoothly with the model simulations in the subtropics where the relaxation is weak. Equation (2) describes  $U_{QBO}$  only up to the 10 hPa level where the Singapore data are available.  $U_{QBO}$  was extended above 10 hPa by assuming a constant downward phase progression of wind anomalies (about 2 km/month) and a fairly rapid drop off in amplitude with height.

[13] One complication of basing  $U_{QBO}$  on the deseasonalized Singapore data, of course, is that the model winds near the equator may be biased in the mean relative to observations. In fact, the SKYHI model climatology near the equator does have an easterly bias relative to Singapore observations, a point which will be apparent when the model simulations are examined below. However, the bias has only small vertical shear relative to the magnitude of the QBO anomaly shears themselves, so the imposed vertical shear (which is related to the QBO temperature perturbations and induced meridional circulations that the model develops in response to the momentum forcing) near the equator is quite representative of the Singapore observations.

[14] Interannual sea-surface temperature variability as well as stratospheric ozone variations can influence changes in the circulation and AO. *Kirchner et al.* [1999] and *Stenchikov et al.* [2002] discussed these effects. However, in this study our goal is to investigate the possibility of different model sensitivity in the easterly and westerly phases of the QBO. After the Pinatubo eruption the QBO phase (as measured by the sign of the 40 hPa prevailing zonal wind) was easterly for the first boreal winter (1991–1992) and westerly for the second winter (1992–1993). In order to isolate these effects, we have to exclude all other time dependent forcings like sea-surface temperature variations and ozone depletion. Therefore calculations were conducted with prescribed climatological sea-surface temperatures and ozone distribution.

[15] One focus of the present study is the extratropical winter circulation, where unforced interannual variability is substantial. To ensure statistical significance of our high-latitude results, ensembles of 24 control and perturbed integrations were conducted. To the best of our knowledge it is the largest ensemble series for this type of study. In particular, 24 control integrations for the period January 1989 to December 1994 were conducted, each starting from different 1 January initial conditions (denoted here as the QBO ensemble (QE) runs). Then the 1 June 1991 results from each of these runs were used as initial conditions in an ensemble of 24 June 1991 to May 1993 integrations with the Pinatubo aerosol (QBO aerosol (QA) runs). In addition, two 22 year (1978–1999) control runs (QBO control (QC)) were conducted.

### 3. Results

[16] We previously simulated the atmospheric effects caused by Pinatubo eruption focusing on the analysis of “tropospheric gradient” and “stratospheric gradient” mechanisms of the AO [*Stenchikov et al.*, 2002]. Both mechanisms are driven by a “wave feedback” caused by an interaction of planetary waves with the polar vortex [*Perlwitz and Graf*, 1995; *Kirchner et al.*, 1999; *Kodera and Kuroda*, 2000a, 2000b; *Shindell et al.*, 2001]. The QBO affects wave feedback in two ways. First, a westerly phase of the QBO strengthens the polar vortex, but an easterly phase weakens it, modulating a refraction of planetary waves in the winter polar stratosphere. Second, in a westerly phase of the QBO, planetary waves in the stratosphere can propagate from the Northern to the Southern Hemisphere through the equator, but in an easterly phase a zero zonal velocity barrier in the tropics prevents propagation of planetary waves from the Northern Hemisphere southward, producing a wave guide between about 10°N and 60°N where wave activity accumulates.

#### 3.1. QBO

[17] First we analyze the QC (long-term control with multiple QBO cycles) and QE (multiple control runs with 1991–1993 QBO cycle) control runs to make sure that the model reproduces the observed QBO circulation when forced as described above (equation (1)). The evolution of the simulated zonal mean zonal wind at the equator extracted from the QC runs compares favorably with the observations from Singapore (Figures 1a and 1b). Figure 1

shows downward propagation of westerlies and easterlies at the equator associated with the QBO. The simulation (Figure 1a) reproduces the observed phase and amplitude of the QBO cycles (Figure 1b), accounting realistically for interannual variations of the stratospheric circulation in tropics. The easterly phase of the QBO in June 1991 to September 1992 was relatively weak, but the westerly phase starting in September 1992 was stronger than average. The simulated westerlies at 20 hPa are stronger than observed (25 m/s versus 20 m/s). The easterlies are slightly underestimated above 50 hPa. Westerlies in the simulation reach only the 60 hPa level and do not descend to 100 hPa as in the observations because of a moderate easterly bias of the model zonal wind  $U_{clim}$  in equation (1) in the 50–100 hPa layer.

[18] Figures 2a and 2b show long-term mean zonal mean zonal wind for winter season DJF from the ensemble QC and from NCEP reanalysis, respectively, both averaged from January 1978 to December 1999. The NCEP data are available only below 20 hPa; therefore winds are not shown above 20 hPa in Figure 2a. The equatorial QBO is averaged out, but polar stratospheric and subtropical tropospheric jets in the Northern Hemisphere are clearly seen. The Northern Hemisphere tropospheric jet in simulations is 5 m/s stronger than observed, but its position compares well with observations. The simulated tropospheric jet in the Southern Hemisphere is 5 m/s weaker than observed and is slightly shifted to south. Tropical winds are simulated fairly well. The model reproduces a somewhat realistic shape and intensity of the polar night jet (Figure 2b). However, zonal winds in the lower stratosphere, especially at the tropopause level, are overestimated.

[19] Figure 3 shows an attempt to isolate the QBO-related temperature anomalies at 50 hPa. Specifically, what is plotted are the zonal mean temperatures averaged over the QE runs for each month from June 1991 to May 1993 minus the long-term mean climatology for the calendar month from the QC runs. The easterly phase of the QBO corresponds with a statistically significant temperature anomaly of about –1 K in the equatorial belt of 15°S–15°N from June 1991 to September 1992. Weaker, but still statistically significant, warm anomalies of up to about 0.5 K extend beyond the equatorial belt to 60°S and 60°N. In the westerly phase, after September 1992, the sign of temperature anomalies is reversed with anomalously warm conditions on the equator and cold anomalies in midlatitudes. While the QBO effect on the temperature in the polar vortex is not large enough in the present 24 simulations to be judged 95% significant, the pattern of temperature anomalies in tropics and midlatitudes is consistent with observations and other model studies [e.g., *Holton and Tan*, 1980, 1982; *Hamilton*, 1998; *Baldwin et al.*, 2001].

#### 3.2. QBO and Aerosols

[20] The QA experiments account for the effects of both the QBO and aerosols. To analyze responses to these forcings, we calculate anomalies with respect to a multiyear average over QC runs (referred below as QA-QC anomalies) and with respect to ensemble average QE runs (referred as QA-QE anomalies). QA-QC anomalies show the combined effect of QBO and aerosols. One can compare QA-QE anomalies here with the anomalies of the aerosol

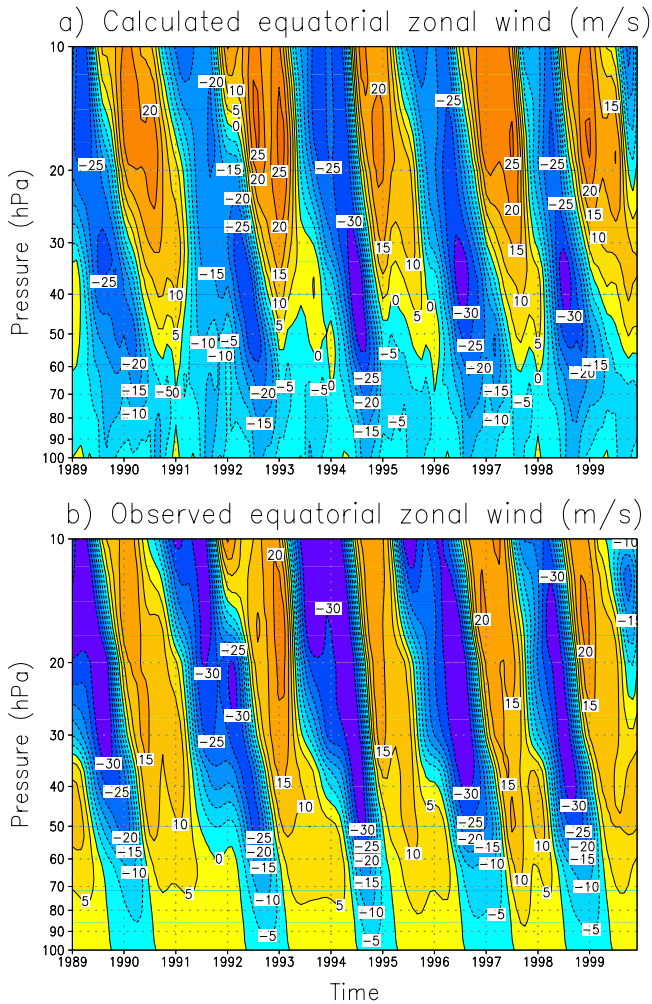


**Figure 1.** (a) Equatorial zonal mean zonal wind (m/s) as a function of pressure and time averaged over ensemble QC and (b) obtained from Singapore observations.

runs versus control runs in the *Stenchikov et al.* [2002] simulations conducted without a QBO.

[21] Figures 4a and 4b show QA-QC and QA-QE zonal mean lower stratospheric temperature anomalies at 50 hPa. With 24 ensemble members the response is statistically significant at the 95% confidence level, not only in low and middle latitudes but also in polar regions from June 1992 through the winter of 1992–1993, when the response is strong. As in simulations without a QBO by *Stenchikov et al.* [2002], the ensemble mean polar stratospheric cooling is weak during the winter of 1991–1992 because the polar vortex was not stable enough and has been broken by polar stratospheric warming in eight of the 24 ensemble simulations. The polar vortex was very strong and stable during the second winter of 1992–1993, producing consistent cooling north of 60°N.

[22] QA-QE polar temperature anomalies (both positive in the first winter and negative in the second) are much stronger than the equivalent aerosol-induced anomalies in the work of *Stenchikov et al.* [2002] without a QBO, pointing to an important nonlinearity in the QBO modulation of the response to the aerosol radiative forcing, at least in polar latitudes. In the tropics, QA-QE anomalies reached

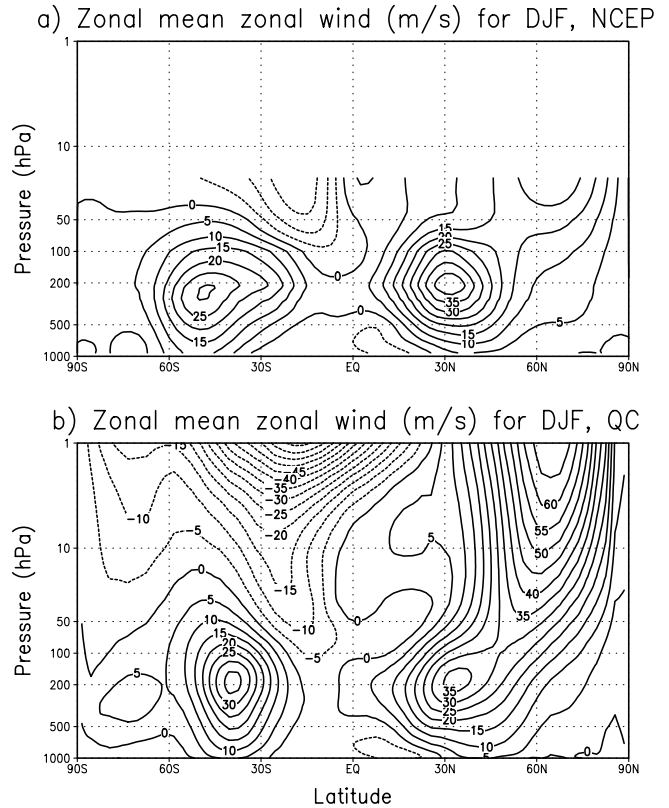


**Figure 2.** Zonal mean zonal wind (m/s) as a function of pressure and latitude for winter season (DJF) averaged over 1978–1999 period calculated using (a) NCEP reanalysis and (b) QC ensemble runs.

about 2 K and from June 1991 to September 1992, which is quite similar to what was obtained by *Stenchikov et al.* [2002] without a QBO, pointing to an almost linear superposition of easterly phase of the QBO and aerosol effects (Figure 4b).

[23] QA-QC zonal mean lower stratospheric temperature anomalies (Figure 4a) for the ensemble mean are compared with the actual observed anomalies in NCEP analyses,

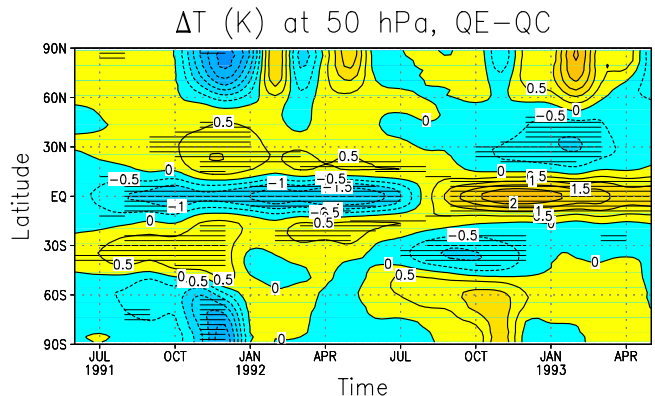


**Figure 3.** Zonal mean lower stratospheric temperature anomalies (K) at 50 hPa for 2 years following the Mt. Pinatubo eruption showing effect of QBO calculated as QE-QC anomalies. The hatching corresponds to a 95% confidence level obtained by a local student's *t* test.

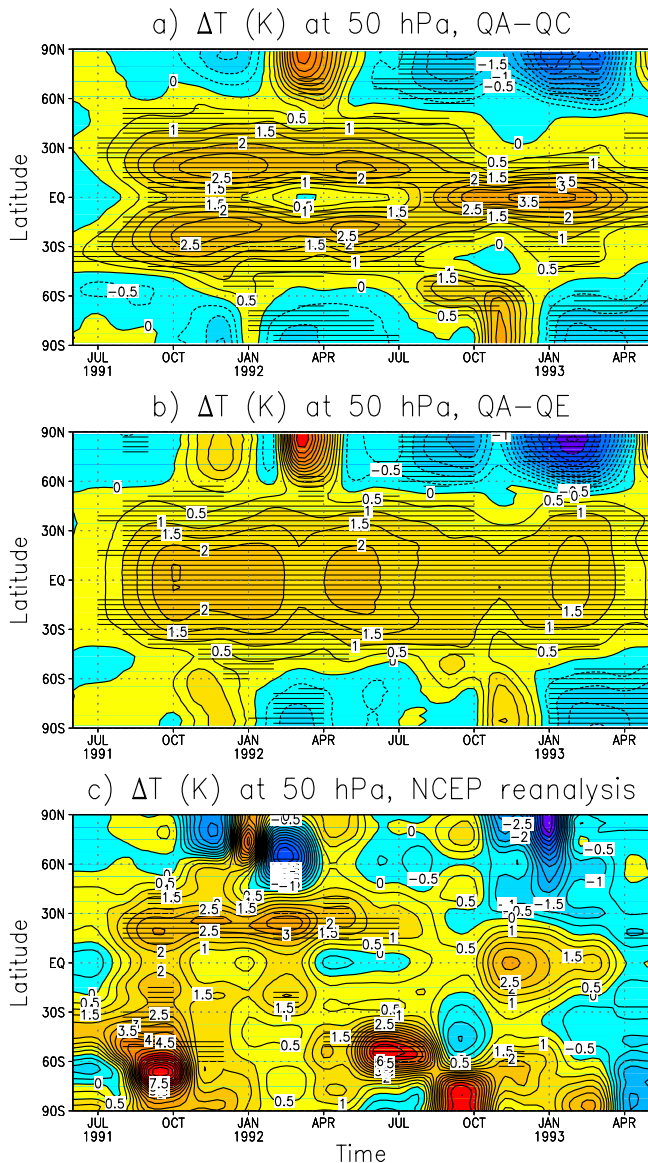


**Figure 4.** Zonal mean lower stratospheric temperature anomalies (K) at 50 hPa calculated from (a) the ensemble QA with respect to climatological multiyear average from QC ensemble and (b) to QE ensemble average for the post-Pinatubo period of June 1991 to May 1993. The hatching corresponds to a 95% confidence level obtained by a local student's  $t$  test. (c) The observed response is calculated from the NCEP reanalysis with respect to the 1985–1990 mean. The hatching corresponds to the 95% confidence level obtained assuming a normal distribution at each grid point and no autocorrelation, with standard deviation calculated using seasonally mean quantities for the period 1951–1990.

where the anomalies are defined as the monthly temperature minus the temperature averaged for the same calendar month over the 5-year period just before the eruption (Figure 4c). In the tropics, there is a very good agreement between the anomalies in the QA-QC simulation and the actual temperature anomalies observed during this period. In the tropical stratosphere, there is relatively little random variation of the zonal mean temperature, and the interannual

variability is dominated by the QBO and any volcanic perturbations. Thus it is meaningful to compare the simulation and single observed realization in some detail. The fact that they agree well suggests that the basic specification of the dynamical QBO and the radiative perturbation associated with the volcanic aerosol are reasonably realistic. The natural variability in the polar lower stratosphere in winter is much higher, and therefore the signal-to-noise ratio is much lower. However, the simulated response (Figure 4a) is qualitatively consistent with observations (Figure 4c) even in high latitudes. For the purpose of this study it is important to emphasize that in simulations the difference between high-latitude temperature anomalies (weak vortex corresponds to warm anomalies and strong vortex corresponds to cold anomalies) in NH in the first and in the second winter affected by the easterly and westerly phase of the QBO, respectively, is statistically significant at 95% confidence level. Further results will demonstrate this point in more detail.

[24] Figure 5 shows QA-QC geopotential height anomalies in the lower stratosphere and in the middle troposphere for each of the 1991–1992 and 1992–1993 winters. Figures 5a and 5b show an anomalously strong stratospheric polar vortex in the first winter of 1991–1992, and a much larger anomaly of the same sign in the second winter of 1992–1993. The geopotential height anomaly in the second winter at high latitudes reaches 140 m. In the absence of the aerosol effect the vortex would be expected to be anomalously weak in the first winter when there is an easterly QBO phase and anomalously strong in the second winter when the QBO is in its westerly phase. The 50 hPa results in Figure 5 could thus be interpreted to first order as the sum of the expected QBO effect and an intensification of the polar vortex due to the aerosol effects. Indeed, *Stenchikov et al.* [2002] found the aerosol effects by themselves lead to a strengthening of the polar vortex. Figures 6a and 6b show the QA-QE anomalies at 50 hPa for the two winters. Interestingly, the QA-QE anomalies in the 1992–1993 winter are almost three times as strong as the aerosol anomalies in the *Stenchikov et al.* [2002] simulations. This suggests that there may be a significant nonlinearity between the QBO and the aerosol effects, with the aerosol strengthening of the vortex being particularly effective when the QBO is in its westerly phase.

[25] The 500 hPa geopotential anomalies are shown for the two winters for QA-QC in Figures 5c and 5d and for QA-QE in Figures 6c and 6d. All the anomalies shown in these figures are consistent with a positive phase of the AO, with negative anomalies in the polar region and positive anomalies in the midlatitudes over North Atlantic, Eurasia, and the west coast of North America. The QA-QC and QA-QE anomalies are fairly similar, suggesting that the direct effect of the QBO on the extratropical middle troposphere is hard to detect, as in observations [Angell, 2001].

[26] Similar to the geopotential height at 500 hPa, QA-QC (Figure 7) and QA-QE (not shown) surface temperature anomalies are not strikingly different. The simulated winter warming pattern is statistically significant at a 95% confidence level over Eurasia but is very weak over North America, as in our previous studies without a QBO. Typical wave pattern of cooling over the Middle East, Africa, and Greenland is well reproduced. The pattern itself is fairly

## Geopotential height anomaly (m), QA–QC

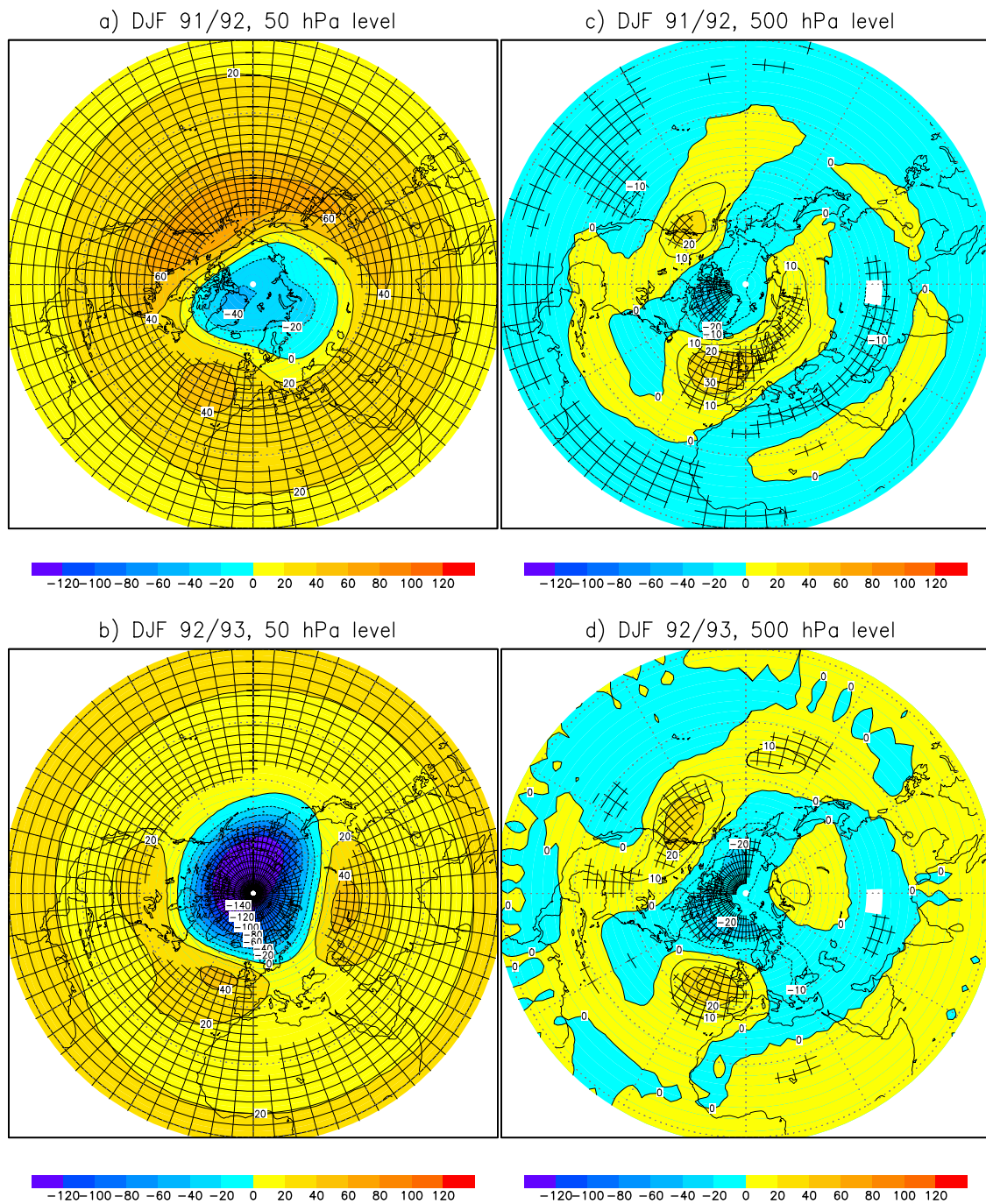


**Figure 5.** Seasonally averaged anomalies of geopotential height (m) at (a and b) 50 hPa and (c and d) 500 hPa obtained from ensemble QA for the winters (DJF) of 1991–1992 and 1992–1993, respectively. Anomalies are calculated with respect to a multiyear mean from the QC runs. The hatching corresponds to a 95% confidence level obtained by a local student's  $t$  test.

similar to what we obtained without a QBO [Stenchikov *et al.*, 2002] but shows a slightly stronger response over North America.

[27] Overall we can conclude that both observed [see Stenchikov *et al.*, 2002, Figures 1–2] and our present simulated tropospheric temperature and circulation responses in the second year are at least as strong as in the first year,

although aerosol radiative forcing declined significantly in the second winter. At the same time the second-year polar vortex was more stable and stronger than in the first year. In the simulations the asymmetry of the response between the two winters is well reproduced. The difference of zonal mean zonal wind between winters of 1992–1993 and 1992–1991 reaches 13 m/s in the Northern Hemisphere

## Geopotential height anomaly (m), QA–QE

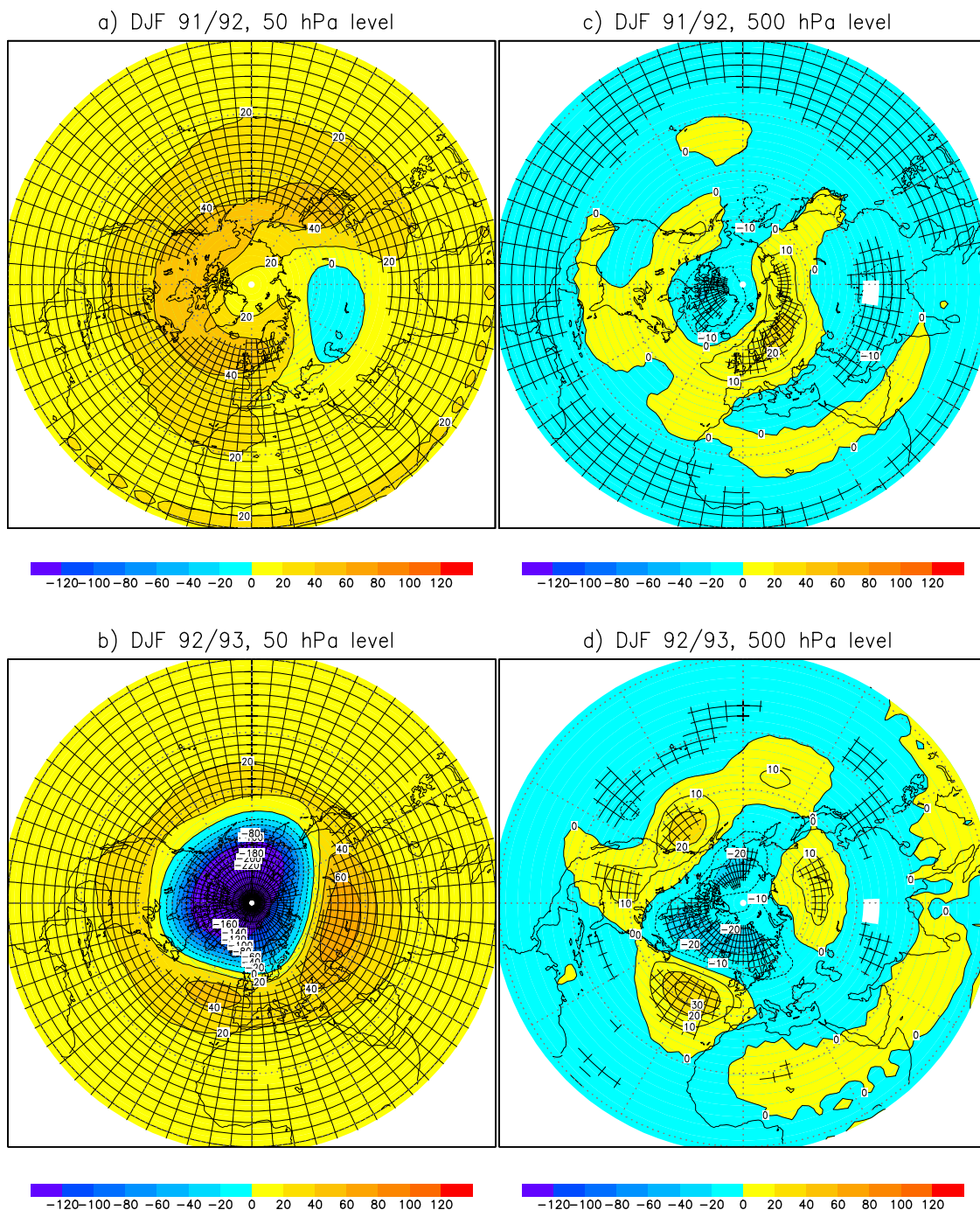


**Figure 6.** Seasonally averaged anomalies of geopotential height (m) at (a and b) 50 hPa and (c and d) 500 hPa obtained from ensemble QA for the winters (DJF) of 1991–1992 and 1992–1993, respectively. Anomalies are calculated with respect to an ensemble mean from the QE runs. The hatching corresponds to a 95% confidence level obtained by a local student's  $t$  test.

extratropics and is statistically significant at 95% confidence level in a wide region of polar stratosphere and upper troposphere (Figure 8a). This result is consistent with observations (Figure 8b).

[28] Neither the *Stenchikov et al.* [2002] simulations with the SKYHI model nor our earlier simulations with another GCM lacking a QBO [*Kirchner et al.*, 1999; *Ramachandran*

*et al.*, 2000] showed a strong amplification of the polar night jet in the second winter after the eruption as our current results do. Therefore we attribute this asymmetry of the response to the strengthening effect of the westerly phase and the weakening effect of the easterly phase of the QBO on the polar vortex. These simulated effects are broadly consistent with observations in the two winters

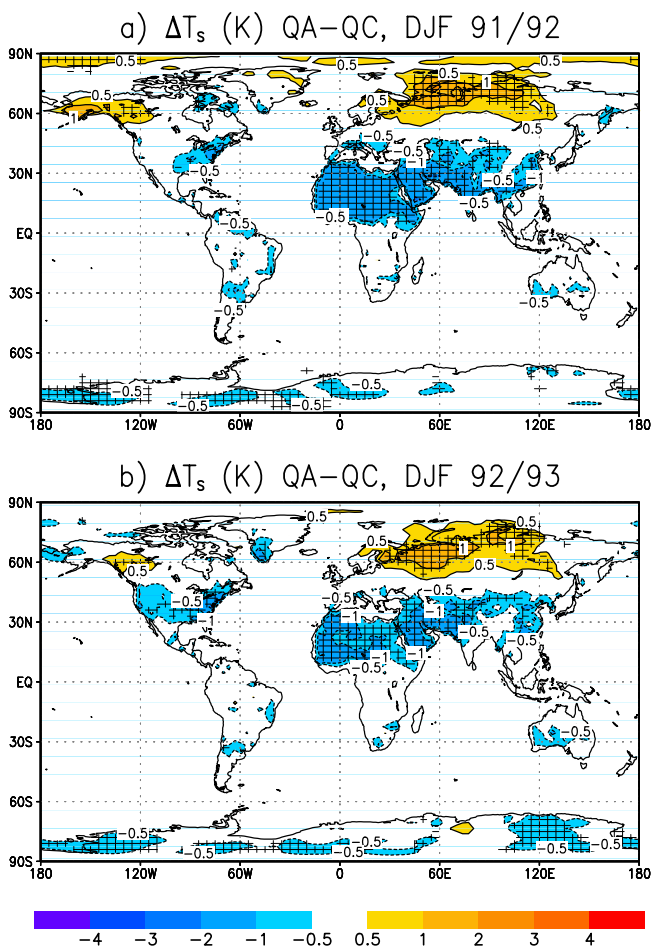


**Figure 7.** Seasonally averaged anomalies of the surface air temperature (K) obtained from ensemble QA for the winters (DJF) of (a) 1991–1992 and (b) 1992–1993. Anomalies are calculated with respect to a multiyear mean from the QC runs. The hatching corresponds to a 95% confidence level obtained by a local student’s *t* test.

following the Mt. Pinatubo eruption and provide a quantification of the QBO effect on the sensitivity of the climate system to an external forcing.

**4. Results in Terms of the Arctic Oscillation**

[29] To analyze the effects of the QBO and aerosol radiative perturbations in terms of the AO, we calculated the first EOF independently for sea-level pressure (SLP) and the geopotential at 500 and 50 hPa for our control runs QC. The data analyzed were December–February means for each year from the last 21 years (1979–1999) of each of the 2 QC runs. Then, following *Thompson and Wallace* [1998], all fields were multiplied by the square root of the cosine of latitude to area-weight contributions of data points from high and low latitudes in the inner product. The first EOF for each of the three levels was calculated in the 20°N–90°N latitude band using GrADS-based routine provided by Matthias Munnich <http://www.atmos.ucla.edu/~munnich/Grads/EOF>. The sign of eigenvectors was chosen to be consistent with the usual definition of the phase of the AO, and they have been normalized so that the standard

deviation of the time series of the amplitude coefficients is 1. The EOF structures are shown in Figure 9. The EOF of 50 hPa geopotential height (Figure 9a) shows strong axisymmetric negative anomalies reaching –50 m in the polar region accompanied by strong positive anomalies in low midlatitudes and tropics. This structure corresponds to an anomalously strong polar vortex. The EOF of geopotential height at 500 hPa (Figure 9b) shows similar but weaker structure. The EOF of SLP (Figure 9c) demonstrates a typical AO distribution with negative pressure anomalies of –2 hPa in the polar region and positive pressure anomalies in midlatitudes and tropics with maxima over Eurasia and Pacific Ocean reaching 1.5 hPa.

[30] In the QC integrations the first EOF of geopotential height at 50 hPa, 500 hPa, and SLP accounts for 35, 18, and 21% of the variance of corresponding fields, respectively. By comparison, *Thompson and Wallace* [1998] found that the first SLP EOF from observations accounts for 22% of the observed variance.

[31] Figure 9d shows the amplitude coefficients for the first EOF in each of the 42 winters from the 2 QC integrations and for each of the three levels. The coefficients

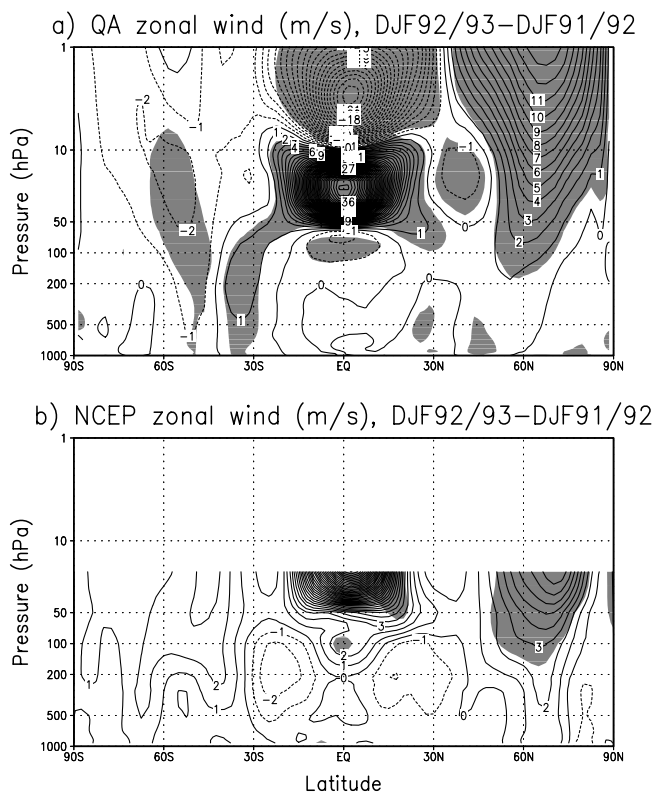


**Figure 8.** (a) The difference of seasonally averaged zonal mean zonal wind (m/s) from ensemble QA between the winters (DJF) of 1992–1993 and 1991–1992. The hatching corresponds to a 95% confidence level obtained by a local student’s *t* test. (b) The difference of seasonally averaged zonal mean zonal wind (m/s) from the NCEP reanalysis between the winters (DJF) of 1992–1993 and 1991–1992. The hatching corresponds to the 95% confidence level obtained assuming a normal distribution at each grid point and no autocorrelation, with standard deviation calculated using seasonally mean quantities for the period 1978–1999.

# First EOFs from QC Runs

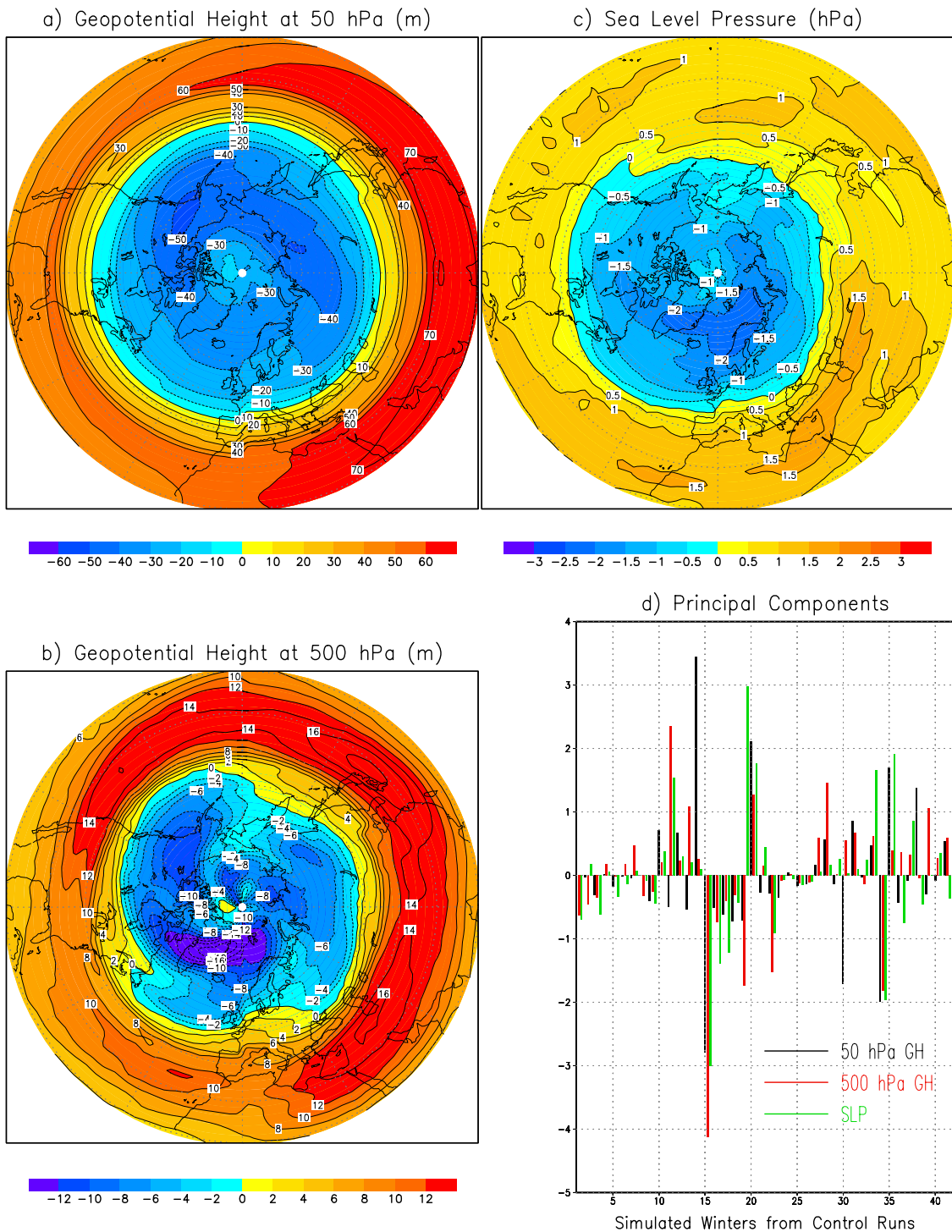


**Figure 9.** First EOFs of geopotential height at (a) 50 hPa (m), (b) 500 hPa (m), and (c) SLP (hPa) obtained from the control ensemble QC for the 42 simulated winters (DJF). (d) Principal components as calculated for 42 individual winters at 50 hPa (black), 500 hPa (red), and SLP (green).

for the control runs are dimensionless, have 0 mean, and, as noted above, the standard deviation equals 1 at all levels. The amplitude coefficients at different levels are well correlated, consistent with the usual view that the AO signal has strong vertical coupling in the troposphere and stratosphere.

[32] The QA-QC anomalies of geopotential height in each winter were projected on the EOFs computed from the control run. Figure 10 shows the resulting amplitude coefficients at each level and for two winters from each of the 24 perturbed runs. These are denoted here as the AO indices for each winter and each level. In individual integrations the

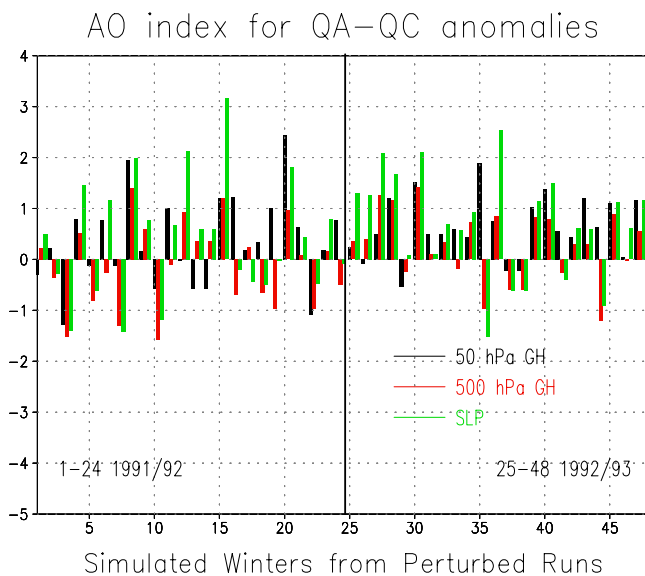


**Figure 10.** AO indexes for 48 individual simulated winters calculated using QA-QC anomalies of geopotential height at 50 hPa (black), geopotential height at 500 hPa (red), and SLP (green).

QA-QC AO index may be positive or negative, but it is evident that the mean over all the simulated seasons is positive and statistically stable because it is not produced by only one or two outliers. In the first column of Table 1 we present the AO indexes averaged for all 48 simulated winters. The indexes are normalized to the standard deviation of 48 ensemble mean (0.14). The results show that volcanic forcing causes on average for 48 winters a positive shift of the AO with 99% confidence level in the lower stratosphere and at the surface but with only 80% confidence level in the middle troposphere. The columns 2–4 in Table 1 present the 24-member ensemble average AO indexes for winters of 1991–1992, 1992–1993, respectively, and their difference for all levels normalized to the standard deviation of 24-member ensemble mean (0.2). In the mean the AO anomalies are stronger in 1992–1993 than in 1991–1992 although, as noted earlier, the radiative forcing is weaker overall in 1992–1993. A positive shift of the AO index in the lower stratosphere and at the surface is especially large in 1992–1993 exceeding the 99% confidence level. This is perhaps an indication of a synergistic effect of the westerly phase of QBO and aerosol forcing.

[33] The simulated difference between AO responses in the first and second winters following the Mt. Pinatubo

eruption is qualitatively similar to observations during the post-Pinatubo period. The observed AO anomalies in winter 1991–1992 and in winter 1992–1993 were both positive, but the anomaly was roughly twice as large in second winter than in the first. Of course, comparison with a single real-world realization in the extratropics has a limited value because of the significant random inter-annual variability present. However, overall the strong tendency for a positive phase of the AO in the two winters following tropical eruptions has support in analysis of observations following numerous major tropical eruptions of the last 150 years [Robock and Mao, 1992, 1995; Kelly et al., 1996].

## 5. Conclusions

[34] We can summarize our findings as follows:

[35] 1. A realistic observed QBO cycle has been successfully implemented in the SKYHI GCM. We were able to realistically simulate the spatial-temporal pattern of the QBO effect on stratospheric temperature and circulation.

[36] 2. An enhanced positive phase of the AO was reproduced in the model in the first and second Northern Hemisphere winters following the eruption when the model was forced with aerosol forcing and QBO.

[37] 3. With aerosols and a QBO the model produced a more realistic spatial-temporal structure of temperature response in the lower stratosphere than in experiments without a QBO. Accounting for the observed phase of the QBO is crucially important to get the right pattern of the lower stratospheric temperature response to volcanic forcing.

[38] 4. The phase of the QBO affects the strengths of the polar vortex and therefore modulates the AO response. The QBO in its easterly phase in the winter of 1991–1992 weakened the polar vortex, amplifying a sudden stratospheric warming at the end of the winter. The westerly phase of the QBO in the winter of 1992–1993 strengthened the polar vortex, causing additional cooling of the Northern Hemisphere polar region and amplifying aerosol effect to produce geopotential height anomalies at 50 hPa three times as large as in simulations without a QBO.

[39] 5. The interaction of aerosols and the QBO is highly nonlinear because of a threshold dependence of planetary wave refraction on the strength of the polar night jet. As a result, aerosols and the westerly phase of the QBO together produce a stronger response than a linear superposition of responses to each of these forcings independently, and aerosols and an easterly phase of the QBO together produce a weaker response than a linear superposition.

**Table 1.** Ensemble Mean AO Indexes for QA-QC Anomalies of Geopotential Height at 50 hPa, 500 hPa, and Sea-Level Pressure (SLP)<sup>a</sup>

Level	Ensemble Mean AO Indexes for QA-QC Anomalies			
	1991–1992 and 1992–1993	1991–1992	1992–1993	1992–1993 Minus 1991–1992
50 hPa	3.43	1.70	3.10	1.40
500 hPa	1.32	0.55	1.30	0.75
SLP	3.78	1.95	3.35	1.40

<sup>a</sup>For column 2 (1991–1992 and 1992–1993) the AO indexes were calculated for all 48 simulated winters and normalized to the standard deviation of the 48 ensemble mean (0.14). For column 3 the AO indexes for the winter of 1991–1992 were normalized to the standard deviation of the 24 ensemble mean (0.20). For column 4 the AO indexes for the winter of 1992–1993 were normalized to the standard deviation of the 24 ensemble mean (0.20). For column 5 the differences between the AO indexes for the winter of 1992–1993 and the winter of 1991–1992 were normalized to the standard deviation of the 24 ensemble mean (0.20).

[40] 6. Increasing the number of ensemble members to 24 improves the statistical significance of the simulated response. However, to make high-latitude anomalies in the lower stratosphere statistically more stable, ensembles with about 50 ensemble members would be desirable.

[41] **Acknowledgments.** We thank Jerry Mahlman, Hans-F. Graf, Judith Perlwitz, and Mark Baldwin for valuable discussions and Larry Polinsky for help in NCEP reanalysis data processing. Supported by NASA grant NAG 5-9792 and NSF grants ATM-9988419 and ATM-0313592.

## References

- Andersen, U. J., E. Kaas, and P. Alpert (2001), Using analysis increments to estimate atmospheric heating rates following volcanic eruptions, *Geophys. Res. Lett.*, **28**, 991–994.
- Andronova, N. G., E. V. Rozanov, F. Yang, M. E. Schlesinger, and G. L. Stenchikov (1999), Radiative forcing by volcanic aerosols from 1850 through 1994, *J. Geophys. Res.*, **104**, 16,807–16,826.
- Angell, J. K. (1997), Stratospheric warming due to Agung, El Chichon, and Pinatubo taking into account the quasi-biennial oscillation, *J. Geophys. Res.*, **102**, 9479–9485.
- Angell, J. K. (2001), Relation of size and displacement of the 300 mbar north circumpolar vortex to QBO, El Nino, and sunspot number, 1963–2000, *J. Geophys. Res.*, **106**, 31,787–31,794.
- Angell, J. K., and J. Korshover (1964), Quasi-biennial variations in temperature, total ozone, and tropopause height, *J. Atmos. Sci.*, **21**, 479–492.
- Baldwin, M. P., and T. J. Dunkerton (1999), Propagation of the arctic oscillation from the stratosphere to the troposphere, *J. Geophys. Res.*, **104**, 30,937–30,946.
- Baldwin, M. P., et al. (2001), The quasi-biennial oscillation, *Rev. Geophys.*, **39**, 179–229.
- Black, R. X. (2002), Stratospheric forcing of surface climate in the Arctic oscillation, *J. Clim.*, **15**, 268–277.
- Bluth, G. J. S., S. D. Doiron, A. J. Krueger, L. S. Walter, and C. C. Schnetzler (1992), Global tracking of the SO<sub>2</sub> clouds from the June 1991 Mount Pinatubo eruptions, *Geophys. Res. Lett.*, **19**, 151–154.
- Bruhwyler, L., and K. Hamilton (1999), A numerical simulation of the stratospheric ozone quasi-biennial oscillation using a comprehensive general circulation model, *J. Geophys. Res.*, **104**, 30,523–30,557.
- Dunkerton, T. J., and M. P. Baldwin (1991), Quasi-biennial modulation of planetary wave fluxes in the Northern Hemisphere winter, *J. Atmos. Sci.*, **48**, 1041–1043.
- Dutton, E. G., and J. R. Christy (1992), Solar radiative forcing at selected locations and evidence for global lower tropospheric cooling following the eruptions of El Chichón and Pinatubo, *Geophys. Res. Lett.*, **19**, 2313–2316.
- Eichelberger, S. J., and J. R. Holton (2002), A mechanistic of the northern annular mode, *J. Geophys. Res.*, **107**(D19), 4388, doi:10.1029/2001JD001092.
- Fels, S. B., J. D. Mahlman, M. D. Schwarzkopf, and R. W. Sinclair (1980), Stratospheric sensitivity to perturbations in ozone and carbon dioxide: Radiative and dynamical responses, *J. Atmos. Sci.*, **37**, 2265–2297.
- Freidenreich, S. M., and V. Ramaswamy (1999), A new multiple band solar radiative parameterization for GCMs, *J. Geophys. Res.*, **104**, 31,389–31,409.
- Fyfe, J. C., G. J. Boer, and G. M. Flato (1999), The Arctic and Antarctic oscillations and their projected changes under global warming, *Geophys. Res. Lett.*, **26**, 1601–1604.
- Graf, H.-F., I. Kirchner, and J. Perlwitz (1998), Changing lower stratospheric circulation: The role of ozone and greenhouse gases, *J. Geophys. Res.*, **103**, 11,251–11,261.
- Groisman, P. Y. (1992), Possible regional climate consequences of the Pinatubo eruption: An empirical approach, *Geophys. Res. Lett.*, **19**, 1603–1606.
- Hamilton, K. (1998), Effects of an imposed quasi-biennial oscillation in a comprehensive troposphere-stratosphere-mesosphere general circulation model, *J. Atmos. Sci.*, **55**, 2393–2418.
- Hamilton, K. (2000), Free and forced interannual variability of the circulation in the extratropical Northern Hemisphere middle atmosphere, in *Atmospheric Science Across the Stratopause*, *Geophys. Monogr. Ser.*, vol. 123, edited by D. E. Siskind, S. D. Eckerman, and M. E. Summers, pp. 227–239, AGU, Washington, D. C.
- Hamilton, K., R. J. Wilson, J. D. Mahlman, and L. J. Umscheid (1995), Climatology of the SKYHI troposphere-stratosphere-mesosphere general circulation model, *J. Atmos. Sci.*, **52**, 5–43.
- Hansen, J. E., et al. (1996), A Pinatubo climate modeling investigation, in *The Mount Pinatubo Eruption: Effects on the Atmosphere and Climate*, NATO ASI Ser., Vol. I, edited by G. Fiocco and G. Visconti, pp. 233–272, Springer-Verlag, New York.
- Hansen, J., R. Ruedy, J. Glasco, and M. Sato (1999), GISS analysis of surface temperature change, *J. Geophys. Res.*, **104**, 30,997–31,022.
- Hoerling, M. P., J. W. Hurrell, and T. Xu (2001), Tropical origins for recent north Atlantic climate change, *Science*, **292**, 90–92.
- Holton, J. R., and H. C. Tan (1980), The influence of the equatorial quasi-biennial oscillation on the global circulation at 50 mb, *J. Atmos. Sci.*, **37**, 2200–2208.
- Holton, J. R., and H. C. Tan (1982), The quasi-biennial oscillation in the Northern Hemisphere lower stratosphere, *J. Meteorol. Soc. Jpn.*, **60**, 140–147.
- Hurrell, J. (1995), Decadal trends in the North Atlantic oscillation: Regional temperatures and precipitation, *Science*, **269**, 676–679.
- Hurrell, J., and H. van Loon (1997), Decadal variations in climate associated with the north Atlantic oscillation, *Clim. Change*, **7**, 1–26.
- Kelly, P. M., and P. D. Jones (1999), Spatial patterns of variability in the global surface air temperature data set, *J. Geophys. Res.*, **104**, 24,237–24,256.
- Kelly, P. M., P. D. Jones, and J. Pengqun (1996), The spatial response of the climate system to explosive volcanic eruptions, *Int. J. Clim.*, **16**, 537–550.
- Kinne, S., O. B. Toon, and M. J. Prather (1992), Buffering of stratospheric circulation by changing amounts of tropical ozone: A Pinatubo case study, *Geophys. Res. Lett.*, **19**, 1927–1930.
- Kinnison, D. E., K. E. Grant, P. S. Connell, and D. A. Rotman (1994), The chemical and radiative effects of the Mount Pinatubo eruption, *J. Geophys. Res.*, **99**, 25,705–25,731.
- Kirchner, I., G. L. Stenchikov, H.-F. Graf, A. Robock, and J. C. Antuña (1999), Climate model simulation of winter warming and summer cooling following the 1991 Mount Pinatubo volcanic eruption, *J. Geophys. Res.*, **104**, 19,039–19,055.
- Kodera, K., and Y. Kuroda (2000a), Tropospheric and stratospheric aspects of the Arctic oscillation, *Geophys. Res. Lett.*, **27**, 3349–3352.
- Kodera, K., and Y. Kuroda (2000b), A mechanistic model study of slowly propagating coupled stratosphere-troposphere variability, *J. Geophys. Res.*, **105**, 12,361–12,370.
- Labitzke, K. (1994), Stratospheric temperature changes after the Pinatubo eruption, *J. Atmos. Terr. Phys.*, **56**, 1027–1034.
- Labitzke, K., and H. van Loon (1995), A note on the distribution of trends below 10 hPa: The extratropical Northern Hemisphere, *J. Meteorol. Soc. Jpn.*, **73**, 883–889.
- Limpasuvan, V., and D. L. Hartmann (1999), Eddies and the annular modes of climate variability, *Geophys. Res. Lett.*, **26**, 3133–3136.
- Lorenz, D. J., and D. L. Hartmann (2003), Eddy-zonal flow feedback in the Northern Hemisphere winter, *J. Clim.*, **16**, 1212–1227.
- Mahlman, J. D., and L. J. Umscheid (1984), Dynamics of the middle atmosphere: Successes and problems of the GFDL SKYHI general circulation model, in *Dynamics of the Middle Atmosphere*, edited by J. R. Holton and T. Matsuno, pp. 501–525, Terra Sci., Tokyo.
- Mahlman, J. D., J. P. Pinto, and L. J. Umscheid (1994), Transport, radiative, and dynamical effects of the Antarctic ozone hole: A GFDL SKYHI model experiment, *J. Atmos. Sci.*, **51**, 489–508.
- McCormick, M. P., and R. E. Veiga (1992), SAGE II measurements of early Pinatubo aerosols, *Geophys. Res. Lett.*, **19**, 155–158.
- Minnis, P., E. F. Harrison, L. L. Stowe, G. G. Gibson, F. M. Denn, D. R. Doeling, and W. L. Smith Jr. (1993), Radiative climate forcing by the Mount Pinatubo eruption, *Science*, **259**, 1411–1415.
- Naujokat, B. (1986), An update of the observed quasi-biennial oscillation of the stratospheric winds over the tropics, *J. Atmos. Sci.*, **43**, 1873–1877.
- Perlwitz, J., and H.-F. Graf (1995), The statistical connection between tropospheric and stratospheric circulation of the Northern Hemisphere in winter, *J. Clim.*, **8**, 2281–2295.
- Polvani, L. M., and P. J. Kushner (2002), Tropospheric response to stratospheric perturbations in a relatively simple general circulation model, *Geophys. Res. Lett.*, **29**(7), 1114, doi:10.1029/2001GL014284.
- Ramachandran, S., V. Ramaswamy, G. L. Stenchikov, and A. Robock (2000), Radiative impacts of the Mt. Pinatubo volcanic eruption: Lower stratospheric response, *J. Geophys. Res.*, **105**, 24,409–24,429.
- Ramaswamy, V., M. D. Schwarzkopf, and W. J. Randel (1996), Fingerprint of ozone depletion in the spatial and temporal pattern of recent lower-stratospheric cooling, *Nature*, **382**, 616–618.
- Randel, W. J., F. Wu, J. M. Russell III, J. W. Waters, and L. Froidevaux (1995), Ozone and temperature changes in the stratosphere following the eruption of Mount Pinatubo, *J. Geophys. Res.*, **100**, 16,753–16,764.
- Randel, W. J., R. S. Stolarski, D. M. Cunnold, J. A. Logan, M. J. Newchurch, and J. M. Zawodny (1999), Trends in the vertical distribution of ozone, *Science*, **285**, 1689–1692.
- Robinson, W. A. (2000), A baroclinic mechanism for the eddy feedback on the zonal index, *J. Atmos. Sci.*, **57**, 415–422.

- Robock, A., and J. Mao (1992), Winter warming from large volcanic eruptions, *Geophys. Res. Lett.*, *19*, 2405–2408.
- Robock, A., and J. Mao (1995), The volcanic signal in surface temperature observations, *J. Clim.*, *8*, 1086–1103.
- Rosenfield, J. E., D. B. Considine, P. E. Meade, J. T. Bacmeister, C. H. Jackman, and M. R. Schoeberl (1997), *J. Geophys. Res.*, *102*, 3649–3670.
- Rozanov, E. V., M. E. Schlesinger, N. G. Andronova, F. Yang, S. L. Malyshev, V. A. Zubov, T. A. Egorova, and B. Li (2002), Climate/chemistry effects of the Pinatubo volcanic eruption simulated by the UIUC stratosphere/troposphere GCM with interactive photochemistry, *J. Geophys. Res.*, *107*(D21), 4594, doi:10.1029/2001JD000974.
- Schoeberl, M. R., P. K. Bhartia, E. Hilsenrath, and O. Torres (1993), Tropical ozone loss following the eruption of Mt. Pinatubo, *Geophys. Res. Lett.*, *20*, 29–32.
- Schwarzkopf, M. D., and S. B. Fels (1991), The simplified exchange method revisited: An accurate, rapid method for computation of infrared cooling rates and fluxes, *J. Geophys. Res.*, *96*, 9075–9096.
- Schwarzkopf, M. D., and V. Ramaswamy (1999), Radiative effects of CH<sub>4</sub>, N<sub>2</sub>O, halocarbons and the foreign-broadened H<sub>2</sub>O continuum: A GCM experiment, *J. Geophys. Res.*, *104*, 9467–9488.
- Shindell, D. T., G. A. Schmidt, R. L. Miller, and D. Rind (2001), Northern Hemisphere winter climate response to greenhouse gas, ozone, solar, and volcanic forcing, *J. Geophys. Res.*, *106*, 7193–7210.
- Solomon, S. (1999), Stratospheric ozone depletion: A review of concepts and history, *Rev. Geophys.*, *37*, 257–316.
- Stenchikov, G. L., I. Kirchner, A. Robock, H.-F. Graf, J. C. Antuña, R. G. Grainger, A. Lambert, and L. W. Thomason (1998), Radiative forcing from the 1991 Mount Pinatubo volcanic eruption, *J. Geophys. Res.*, *103*, 13,837–13,857.
- Stenchikov, G., A. Robock, V. Ramaswamy, M. D. Schwarzkopf, K. Hamilton, and S. Ramachandran (2002), Arctic oscillation response to the 1991 Mount Pinatubo eruption: Effects of volcanic aerosols and ozone depletion, *J. Geophys. Res.*, *107*(D24), 4803, doi:10.1029/2002JD002090.
- Thompson, D. W. J., and J. M. Wallace (1998), The Arctic oscillation signature in the wintertime geopotential height and temperature fields, *Geophys. Res. Lett.*, *25*, 1297–1300.
- Thompson, D. W. J., and J. M. Wallace (2000), Annular modes in the extratropical circulation, I, Month-to-month variability, *J. Clim.*, *13*, 1000–1016.
- Thompson, D. W. J., M. P. Baldwin, and J. M. Wallace (2001), Stratospheric connection to Northern Hemisphere wintertime weather: Implications for prediction, *J. Clim.*, *15*, 1421–1428.
- Turco, R. P., K. Drdla, A. Tabazadeh, and P. Hamill (1993), Heterogeneous chemistry of polar stratospheric clouds and volcanic aerosols, in *The Role of the Stratosphere in Global Change, NATO ASI Ser.*, vol. 8, edited by M.-L. Chanin, pp. 65–134, Springer-Verlag, New York.
- Wetherald, R. T., and S. Manabe (1988), Cloud feedback processes in a general circulation model, *J. Atmos. Sci.*, *45*, 1397–1415.

---

K. Hamilton, International Pacific Research Center, University of Hawaii, Honolulu, HI 96822, USA.

V. Ramaswamy and M. D. Schwarzkopf, NOAA Geophysical Fluid Dynamics Laboratory, Princeton University, P.O. Box 308, Forrestal Campus, Route 1, Princeton, NJ 08452, USA.

A. Robock and G. Stenchikov, Department of Environmental Sciences, Rutgers University, 14 College Farm Road, New Brunswick, NJ 08901-8551, USA. (gera@envsci.rutgers.edu)